MDPI

*Article*

# Cation Exchange Membranes Coated with Polyethyleneimine and Crown Ether to Improve Monovalent Cation Electrodialytic Selectivity

Shanshan Yang [1], Shuaijun Yu [1], Lu Yu [1], Yuanwei Liu [2], Junbin Liao [1], Jiangnan Shen [1,*] and Congjie Gao [3]

[1] College of Chemical Engineering, Zhejiang University of Technology, Hangzhou 310014, China; yangss97@163.com (S.Y.); finesnow2021@163.com (S.Y.); yulu8823@163.com (L.Y.); jbliao@zjut.edu.cn (J.L.)
[2] Department of Chemical Engineering and Safety, Binzhou University, Binzhou 256600, China; hbgfz@163.com
[3] Center for Membrane and Water Science & Technology, Zhejiang University of Technology, Hangzhou 310014, China; gaocj@zjut.edu.cn
* Correspondence: shenjn@zjut.edu.cn

**Abstract:** Developing monovalent cation permselective membranes (MCPMs) with high-efficient permselectivity is the core concern in specific industrial applications. In this work, we have fabricated a series of novel cation exchange membranes (CEMs) based on sulfonated polysulfone (SPSF) surface modification by polyethyleneimine (PEI) and 4′-aminobenzo-12-crown-4 (12C4) codeposited with dopamine (DA) successively, which was followed by the cross-linking of glutaraldehyde (GA). The as-prepared membranes before and after modification were systematically characterized with regard to their structures as well as their physicochemical and electrochemical properties. Particularly, the codeposition sequence of modified ingredients was investigated on galvanostatic permselectivity to cations. The modified membrane (M-12C4-0.50-PEI) exhibits significantly prominent selectivity to Li$^+$ ions ($P_{Mg^{2+}}^{Li^+}$ = 5.23) and K$^+$ ions ($P_{Mg^{2+}}^{K^+}$ = 13.56) in Li$^+$/Mg$^{2+}$ and K$^+$/Mg$^{2+}$ systems in electrodialysis (ED), which is far superior to the pristine membrane (M-0, $P_{Mg^{2+}}^{Li^+}$ = 0.46, $P_{Mg^{2+}}^{K^+}$ = 1.23) at a constant current density of 5.0 mA·cm$^{-2}$. It possibly arises from the synergistic effects of electrostatic repulsion (positively charged PEI), pore-size sieving (distribution of modified ingredients), and specific interaction effect (12C4 ~Li$^+$). This facile strategy may provide new insights into developing selective CEMs in the separation of specific cations by ED.

**Keywords:** electrodialysis; monovalent cation permselectivity; codeposition; polyethyleneimine; 4′-aminobenzo-12-crown-4

## 1. Introduction

With the development of the economy and degradation of the environment, water crisis has become a worldwide problem. Considerable attention has been focused on the ion exchange membrane (IEM) in water purification, brackish-water desalination, demineralization, and wastewater treatment to meet green processes [1–5]. Furthermore, in specific water treatment processes, the development of IEMs with high-efficient permselectivity between counter-ions of different valences or the same valences is of significant importance, such as lithium extraction from high Mg$^{2+}$/Li$^+$ ratio salt-lake brine [6], acid recovery in hydrometallurgy, and the removal of F$^-$ or NO$_3{}^-$ from groundwater [7,8].

In regard to cation exchange membrane (CEM), improving the permselectivity of monovalent cations can be achieved generally through three physicochemical effects: pore-size sieving, electrostatic repulsion, and specific interaction effects [5,9]. Following the pore-size sieving effect, the improvement of cross-linking degree [10,11] and formation of hydrophilic/hydrophobic separated structures [12–14] are the main approaches of altering the structures of membrane matrix to realize cation permselectivity. According to numerous reported studies, surface modification is considered as a facile and efficient

approach to prepare monovalent cation permselective membranes (MCPMs). A series of cationic polyelectrolytes are usually utilized as functional modified materials, such as polypyrrole [15,16], polyaniline [17,18], polyethyleneimine (PEI) [19,20], polyquaternium-7 [21], chitosan, and its derivatives [22,23], which are decorated on the membrane surface through physical or chemical interaction.

Wang et al. reported a three-step modification scheme to covalently immobilize PEI multilayers on commercial heterogeneous CEMs, and the membranes presented superior monovalent selectivity in $Na^+/Mg^{2+}$ and $H^+/Zn^{2+}$ systems based on electrostatic repulsion effect [20]. Similarly, sulfonated poly(ether sulfone) (SPES) CEMs codeposited by PEI and dopamine (DA) presented 2.5 times higher permselectivity to $H^+$ ions than SPES in a $H^+/Zn^{2+}$ system proposed by Li et al. [24]. Gohil et al. developed MCPMs by the oxidation polymerization of pyrrole on the CEM surface, and the tight and rigid polypyrrole layer achieved efficient separation of mono/bivalent cations [16]. In addition, Thakur et al. designed a novel modified method through controlled metal (Cu) loading on poly(2-acrylamido-2-methyl-propane-sulfonic acid) CEM by electro-less plating, and the optimized membrane exhibited extremely low $Zn^{2+}$ leakage owing to the excellent pore-size sieving effect [25]. A series of CEMs modified by chitosan hydrochloride according to electrodepositing and coating respectively achieved high-efficient $Na^+/Mg^{2+}$ separation in optimized conditions, which depended on the synergetic effect of pore-size sieving and electrostatic repulsion [26]. Based on this synergetic effect, Pang et al. prepared novel modified sulfonated polyphenylsulphone (SPPSU) CEMs by in situ polymerization-deposited polyaniline followed by quaternizing with methyl iodide and the adjustment of positive charge density of the modification layer by controlling the degree of quaternization leading to prominent permselectivity for the $Na^+/Mg^{2+}$ and $Li^+/Mg^{2+}$ mixture [27]. In our previous work, the modification of a sulfonated polysulfone (SPSF) membrane through the codeposition of DA and 4′-aminobenzo-15-crown-5 (ACE) followed by GA cross-linking was beneficial to achieve pronounced $K^+$ ions electrodialytic selectivity. Apart from pore-size sieving effect, the electric field driving and host–guest molecular recognition of ACE and $K^+$ ions are essentially taken into account in evaluation of membrane permselectivity [28].

As a large ring organic compound with a polyether structure, crown ether possesses a nanoscale cavity structure, and it can bind specific metal ions to form a stable complex through electrostatic interactions [29,30], which can offer channels for specific ions. As is known, the cavity of 12-crown-4-ether (internal diameter 1.2–1.5 Å) just matches the diameter of a $Li^+$ ion (1.2 Å) and they can form a 1:1 host–guest complexation [31,32]. Ali et al. reported a nanofluidic device for specific $Li^+$ recognition via host–guest complexation between aminoethyl-benzo-12-crown-4 and $Li^+$ in a confined environment [33]. In addition, PEI possesses a hyperbranched structure and abundant positively charged amine groups so that it is widely applied in membrane fabrication and modification [24,34].

Keeping in view the above findings, we proposed a novel modification means of combining positively charged PEI with 4′-aminobenzo-12-crown-4 (12C4) with the ability to recognize specific cations. Based on the inherent adhesion virtues of DA, sulfonated polysulfone (SPSF) CEMs were modified by the two-time codeposition of 12C4/DA and PEI/DA successively through Michael addition or Schiff base reaction [35], followed by the cross-linking of GA. The modified membranes have been characterized regarding the physicochemical and electrochemical properties. Furthermore, we have systematically investigated and analyzed the codeposition sequence of modified ingredients on galvanostatic permselectivity to cations in binary systems of $Li^+/Mg^{2+}$, $K^+/Mg^{2+}$, and $K^+/Li^+$.

## 2. Experimental Section

### 2.1. Materials

Sulfonated polysulfone (SPSF, the molar percent of bis(4–fluorophenyl) sulfone with respect to the total molar of difluoro monomers bis(4–fluorophenyl) sulfone and sul-

fonated bis(4–fluorophenyl) sulfone used in the synthesis procedure was 60%, Mw = 65,000, PDI = 2.25, Yanjin Technology Co., Ltd., Tianjin China), dopamine hydrochloride (98%, Aladdin Reagent Co., Ltd., Shanghai, China), benzo-12-crown-4 (98%, Meryer (Shanghai) chemical Technology Co., Ltd., Shanghai, China), polyethyleneimine (PEI, Mw = 10,000 Da, Aladdin Reagent Co., Ltd., Shanghai, China), glutaraldehyde (GA, 50% in water, Energy Chemical Co., Ltd., Shanghai, China), Tris(hydroxymethyl) aminomethane (Tris, 99.5%, Energy Chemical Co., Ltd., Shanghai, China), $N,N$-dimethylformamide (DMF, 99.5%), chloroform (99%), hydrogen peroxide ($H_2O_2$, 30% by weight), concentrated nitric acid ($HNO_3$, 68%), acetic acid (HAc, 98%), lithium chloride (LiCl, 99.9%), potassium chloride (KCl, 99.5%), magnesium chloride ($MgCl_2$, 99%), sodium sulfate ($Na_2SO_4$, 99.0%), and copper sulfate ($CuSO_4 \cdot 5H_2O$, 99%) were received from Aladdin Reagent Co., Ltd. (Shanghai, China) and used without further purification. Deionized (DI) water was used throughout the experiments.

### 2.2. Membrane Fabrication

The procedures of SPSF-based CEM were carried out as follows: 10 g of SPSF was dissolved in 30 g of DMF solvent and mechanically stirred at 60 °C for 4 h. The homogeneous casting solution was cast on a glass plate with a thickness of 700 μm, which was followed by solvent evaporation at 60 °C. The obtained membrane was stored in DI water for use.

### 2.3. Surface Modification of the Membranes

4′-Aminobenzo-12-crown-4 (12C4) was synthesized according to the preparation of 4′-aminobenzo-15-crown-5 in our previously reported work [28]. PEI and 12C4 were respectively codeposited with DA by means of rapid deposition using $CuSO_4/H_2O_2$ as a trigger [36]. In detail, PEI/DA codeposition solution was carried out as follows: 0.1 g of PEI, 0.2 g of dopamine hydrochlofide and 0.125 g of $CuSO_4 \cdot 5H_2O$ were dissolved in 100 mL of Tris–HCl buffer solution (pH ~8.5, 10 mM) followed by addition of 0.2 mL of $H_2O_2$. 12C4/DA codeposition solution was formed similar to PEI/DA solution. Instead of PEI, 12C4 was added in the aforementioned buffer solution with a designed molar ratio of 12C4/DA (0.50:1 and 0.75:1).

The modified processes on the membrane surface are shown in Figure 1. The circular pieces of CEMs with diameter of 6 cm were horizontally fixed in the holder. The upper surface of membrane was immersed into the fresh prepared 12C4/DA codeposition solution for 6 h at 25 °C and then transferred into PEI/DA codeposition solution for 6 h. Afterward, the modified membranes were washed by DI water for several times and cross-linked by 2.5 wt % GA of aqueous solution for 30 min at 50 °C. Finally, the obtained membranes were rinsed three times and stored in DI water for further characterization and evaluation. For convenience, the aforementioned modified membranes were denoted as M-12C4-x-PEI (x = 0.50 and 0.75). Another group of membranes was successively modified by PEI/DA and 12C4/DA co-deposition solution and further cross-linked, which was denoted as M-PEI-12C4-x (x = 0.50 and 0.75). For comparison, a series of membranes were only modified by PEI/DA or 12C4/DA under the same conditions and they were respectively referred to as M-PEI and M-12C4-x (x = 0.50 and 0.75).
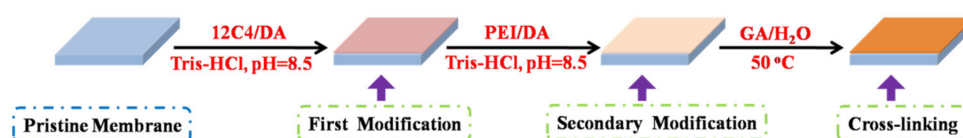


**Figure 1.** Schematic illustrations of the modified processes on SPSF membrane surface.

### 2.4. Membrane Characterization

#### 2.4.1. Structure and Morphology Characterization

The chemical structures of membrane surfaces were measured by attenuated total reflectance Fourier transform infrared spectrophotometer (FT-IR, Nicolet 6700, Waltham,

MA, USA). Spectra of dried samples were collected in the range of 400–4000 cm$^{-1}$. Semi-quantitative analysis of chemical components was investigated by X-ray photoelectron spectroscopy (XPS) on a spectrometer (Thermo Fischer ESCALAB 250XI, Waltham, MA, USA) with Al Kα excitation radiation (1486.6 eV). The scanning electron microscope (SEM, SU8010 Hitachi, Tokyo, Japan) was used to observe the elements distribution in cross-section of the CEMs. The samples were dried in a freeze dryer for more than 24 h before characterization.

### 2.4.2. Ion Exchange Capacity (IEC)

Ion exchange capacity of CEMs was determined by acid–base titration. Pieces of dry CEMs ($W_{dry}$, g) were soaked in 25 mL of 1.0 M HCl solution for 48 h to convert all charge sites in membrane matrix into the H$^+$ form and then washed with DI water to remove the residual H$^+$ on the membrane surface. Subsequently, the membranes were immersed in 25 mL of 0.5 M NaCl solution for 48 h to release H$^+$ ions in membrane matrix. The remaining solution was titrated against NaOH solution with a known concentration ($c_{NaOH}$, mol·L$^{-1}$) using phenolphthalein as the indicator. The equivalent volume of NaOH was denoted as $V_{NaOH}$ (mL). The IEC (mmol·g$^{-1}$) value was calculated by Equation (1):

$$IEC = \frac{c_{NaOH} \times V_{NaOH}}{W_{dry}}. \tag{1}$$

### 2.4.3. Water Uptake

Water uptake (WU) refers to the weight difference after the membrane is fully hydrated, relative to the dry membrane. Before hydrated, membrane samples were dried to constant weight under vacuum and weighed ($W_{dry}$, g). Then, samples were immersed in water to reach equilibrium at 25 °C. The excess moisture on membrane surface was wiped with filter paper; then, the wet membrane sample was immediately weighed ($W_{wet}$, g). WU was calculated as per Equation (2):

$$WU = \frac{W_{wet} - W_{dry}}{W_{dry}} \times 100\%. \tag{2}$$

### *2.5. Electrochemical Characterization*

### 2.5.1. Surface Area Resistance

The surface area resistance ($R$) of the as-prepared CEMs was measured by a custom-designed four-compartment cell and calculated according to electrochemical impedance spectroscopy (EIS) recorded by an Autolab electrochemical workstation (PGSTAT302 N, Metrohm, Herisau, Switzerland). As shown in Figure 2, the measurement was performed according to our published work [28]. In the four-compartment cell, the CEM to be tested was clamped in the middle two compartments filled with 0.5 M chloride salt solution (LiCl and MgCl$_2$, respectively), and two pieces of AEMs were placed respectively on both ends of the compartments full of 0.5 M Na$_2$SO$_4$. The cathode and anode made of titanium coating ruthenium were utilized as the working electrode (WE) and counter electrode (CE), respectively. A couple of saturated Ag/AgCl electrodes, as the reference electrode (RE) and sensitive electrode (SE), were placed on both sides of the tested membrane as closely as possible. EIS was measured with an AC signal of 10 mV amplitude and the frequency ranging from 103 kHz to 100 mHz at room temperature. $R_i$ (Ω·cm$^2$) was calculated as follows:

$$R_i = (|Z|_m - |Z|_n) \times S_m \tag{3}$$

where $|Z|_m$ and $|Z|_n$ represent the impedance value with and without the tested CEM, $S_m$ is the effective membrane area (7.065 cm$^2$) in this setup, and *i* represents electrolyte species.
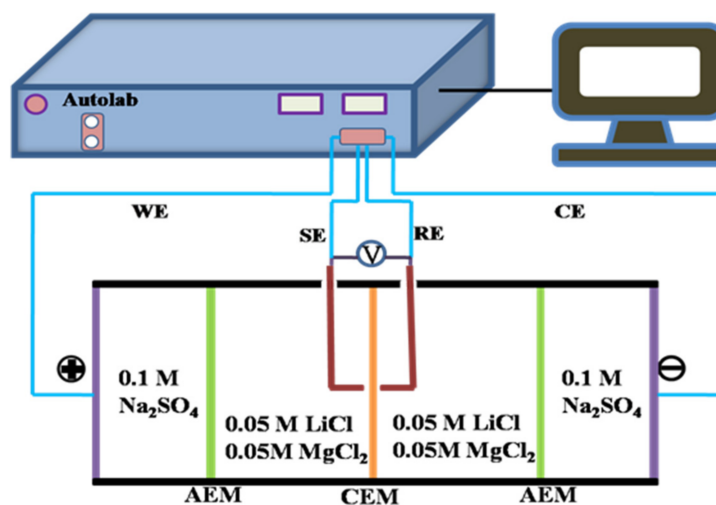
**Figure 2.** Schematic diagrams of the experimental setup for the measurement of EIS and polarization current–voltage curves.

### 2.5.2. Current–Voltage test

Current–voltage curves were measured on a four-electrode setup (see the diagram in Figure 2), similar to $R_i$ measurement described above. The DC current was supplied with a scan rate of 250 $\mu A \cdot s^{-1}$. During the measurement, the electrode solution was 0.1 M $Na_2SO_4$ solution, and the work solution was the mixture of 0.05 M LiCl and 0.05 M $MgCl_2$.

### 2.5.3. Monovalent Cation Selectivity

ED experiments were performed in a homemade four-compartment setup to measure the membrane permselectivity ($Li^+/Mg^{2+}$) under galvanostatic condition at room temperature. The assembly of the device was shown in Figure 3, containing the dilute (DC), the concentrate (CC), and two electrode compartments. The electrode compartments were circulated with 0.1 M $Na_2SO_4$ solution. The DC and CC were both filled with 80 mL of 0.05 M equimolar binary mixtures of chloride salts ($Li^+/Mg^{2+}$, $K^+/Mg^{2+}$, $K^+/Li^+$), to avoid the influence of concentration gradients in these compartments. Concentration of the cations in the DC and CC was determined by Cation Chromatography (ICS-1100, Thermo Fisher, Waltham, MA, USA) at 60 min. The flux of the target cation was determined by its concentration change ($mol \cdot L^{-1}$) in the CC as per Equation (4):

$$J_i = \frac{V}{A_m}\left(\frac{dc_i}{dt}\right) \tag{4}$$

where $J_i$ is the flux of cation ($i$) through the CEM ($mol \cdot m^{-2} \cdot s^{-1}$), $V$ is the volume (L) of electrolyte in the CC (volume change was negligible within a certain time), and $A_m$ is the effective area (19.625 $cm^2$) of the tested CEM.

The permselectivity of CEM between $A^{m+}$ and $B^{n+}$ (denoted as $P_{B^{n+}}^{A^{m+}}$) was generally defined by the following Equation (5).

$$P_{B^{n+}}^{A^{m+}} = \frac{t_{A^{m+}}/t_{B^{n+}}}{c_{A^{m+}}/c_{B^{n+}}} = \frac{J_{A^{m+}} \cdot c_{B^{n+}}}{J_{B^{n+}} \cdot c_{A^{m+}}} \tag{5}$$

where $t_{A^{m+}}$ and $t_{B^{n+}}$ are the transport numbers of $A^{m+}$ and $B^{n+}$ in the membrane phase, $c_{A^{m+}}$ and $c_{B^{n+}}$ are the concentrations ($mol \cdot L^{-1}$) of $A^{m+}$ and $B^{n+}$ in the DC during ED, respectively. $J_{A^{m+}}$ and $J_{B^{n+}}$ represent the fluxes ($mol \cdot m^{-2} \cdot s^{-1}$) of $A^{m+}$ and $B^{n+}$ through the membrane.
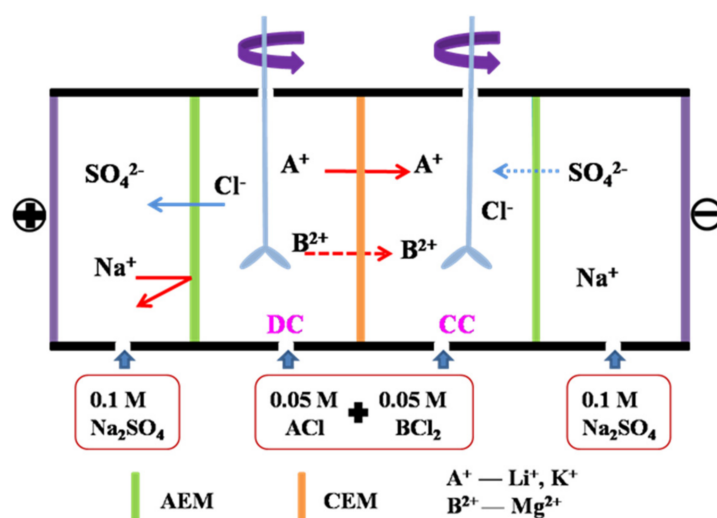
**Figure 3.** Schematic ED apparatus for the measurement of cation permselectivity for the pristine and modified membranes.

Current efficiency ($\eta$, %) and the special energy consumption ($E_{SEC}$, kWh/mol $A^{m+}$, $A^{m+}$ is the target cation) in the process of ED were calculated according to the Reference [37], as shown in Equations (6) and (7).

$$\eta(\%) = \frac{(n_t - n_0)zF}{N\int_0^t I(t)dt} \times 100 \tag{6}$$

$$E_{SEC}(kWh/mol A^{m+}) = \frac{I\int_0^t U(t)dt}{n_R} \tag{7}$$

where $n_t$ and $n_0$ are the number of moles of $A^{m+}$ at time $t$ and initial condition in the CC; $z$ is the valance of $A^{m+}$; $F$ is the Faraday constant (96485 C/mol); $I$ is the constant current (0.1 A) and $t$ is 60 min; $N$ is the number of repeating units ($N = 1$); $U$ is the detected voltage (V) during the ED process; $n_R$ represents the molar number of $A^{m+}$ increased in the CC.

## 3. Results and Discussions

### 3.1. Chemical Structures and Compositions of the Membrane Surfaces

FT-IR was used to analyze the chemical structures of the membrane surfaces for the pristine and modified membranes, and the spectra are exhibited in Figure 4. The obvious characteristic peaks at 1026 and 1096 cm$^{-1}$ in all of the spectra (a)–(e) are assigned to the symmetric and asymmetric stretching vibrations of the sulfonated group [28,38]. A broad band around 3460 cm$^{-1}$ is ascribed to the stretching vibration of the O-H bond in the sulfonated group and residual moisture in the membrane matrix. The newly developed peaks at 1530 cm$^{-1}$ and 3207 cm$^{-1}$ that emerged in spectra (b)–(e), respectively corresponded to the N–H shearing vibration and stretching vibration derived from PDA, PEI, and 12C4 [39,40]. An additional peak arises at 1106 cm$^{-1}$, which is ascribed to the C–N stretching vibration in PDA, PEI, and 12C4 of the modified layers [41]. In order to further certify the element composition on membrane surfaces, XPS analysis was measured, and the results are displayed in Table 1. In comparison with M–DA, the C/O ratio slightly increases from 3.42 to 3.73, and the O/N ratio significantly increases from 4.30 to 6.01 for M-12C4-0.75, owing to the higher ratio of O element (23.53%) than that of N element (5.88%) in 12C4 molecule. After further codepositing of PEI/DA on the membrane surface for M-12C4-0.75-PEI, a sharply decreased ratio of O/N is mainly attributed to N content of PEI molecule. Compared with M-12C4-0.75-PEI, the increased C/N ratio for M-PEI-12C4-0.75 is derived from the higher C/N ratio in 12C4 than that in PEI.
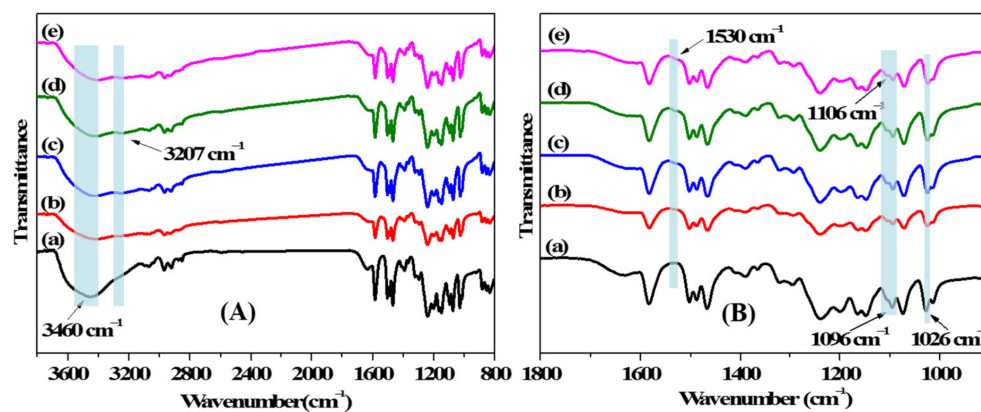
**Figure 4.** FT-IR spectra of membranes (a) M-0, (b) M-12C4-0.75, (c) M-PEI, (d) M-12C4-0.75-PEI, and (e) M-PEI-12C4-0.75 in (**A**) and (**B**) with different wavenumber ranges.

**Table 1.** Chemical composition of the pristine (M-0) and modified (M-DA, M-12C4-0.75, M-12C4-0.75-PEI, and M-PEI-12C4-0.75) membranes surface from XPS spectra.

| Materials/Membranes | C (%) | O (%) | N (%) | S (%) | C/O | C/N | O/N |
|---|---|---|---|---|---|---|---|
| DA (theoretical) | 72.73 | 18.18 | 9.09 | | 4.00 | 8.00 | 2.00 |
| PEI (theoretical) | 66.67 | | 33.33 | | | 2.00 | |
| 12C4 (theoretical) | 70.59 | 23.53 | 5.88 | | 3.00 | 12.00 | 4.00 |
| M-0 | 76.39 | 20.08 | | 3.53 | 3.80 | | |
| M-DA | 71.95 | 21.06 | 4.90 | 2.09 | 3.42 | 14.68 | 4.30 |
| M-12C4-0.75 | 74.88 | 20.05 | 3.34 | 1.73 | 3.73 | 22.45 | 6.01 |
| M-12C4-0.75-PEI | 76.62 | 18.90 | 3.67 | 0.82 | 4.05 | 20.90 | 5.16 |
| M-PEI-12C4-0.75 | 78.77 | 17.46 | 3.08 | 0.69 | 4.51 | 25.56 | 5.66 |

### 3.2. Physicochemical Properties

IEC represents the exchangeable ionic sites and sheds light on the ionic conductivity and water absorption in membrane matrix. WU reveals the proportion of the hydrophilic domains in the membrane matrix and influences the ion transportation. IECs and WUs of the pristine and modified membranes are displayed in Figure 5. In general, IEC and WU values of modified membranes almost decrease compared with M-0. The IECs of M-12C4-0.50 and M-12C4-0.75 are respectively 1.89 and 1.83 mmol·g$^{-1}$, while the values gradually fall down to 1.70 and 1.66 mmol·g$^{-1}$ for M-12C4-0.50-PEI and M-12C4-0.75-PEI. From the EDX mapping of the N element in the whole cross-section of M-12C4-0.75-PEI (see Figure 6b), we can see that the distribution of the N element is almost uniform. It can confirm the permeation of codeposition solution (12C4/DA and PEI/DA) to the membrane matrix easily. During the 12C4/DA codeposited reaction, 12C4 and DA gradually permeate into the membrane matrix, and the amine groups mainly from PDA interact with sulfonate groups in the membrane matrix, leading to decreased exchangeable sites [28,42]. The further variation of IECs for M-12C4-x-PEI (x = 0.50 and 0.75) is plausibly attributed to the acid–base interaction between sulfonate groups and DA small molecules in PEI/DA codeposition solution. Furthermore, a secondary modified layer of PEI/DA was coated on the membrane surface, leading to a relatively thicker layer. Indeed, WU of M-12C4-0.75-PEI decreases to 18.15% compared with M-12C4-0.75 (26.86%). It confirms that modified medium occupies abundant free space of the membrane matrix [43]. The IEC of M-PEI is 1.76 mmol·g$^{-1}$; similarly, it drops to 1.56 mmol·g$^{-1}$ for M-PEI-12C4-0.75. Amine groups derived from positive PEI on the membrane surface and DA permeated into the membrane phase contacted with sulfonate groups inherent in the membrane, resulting in lower exchangeable sites. Furthermore, a secondary coating of 12C4/DA not only seriously reduces IECs but also leads to lower WUs for M-PEI-12C4-0.50 (0.75). This should be

attributable to the greater accumulation of modified medium in the membrane matrix and thicker modified layers.
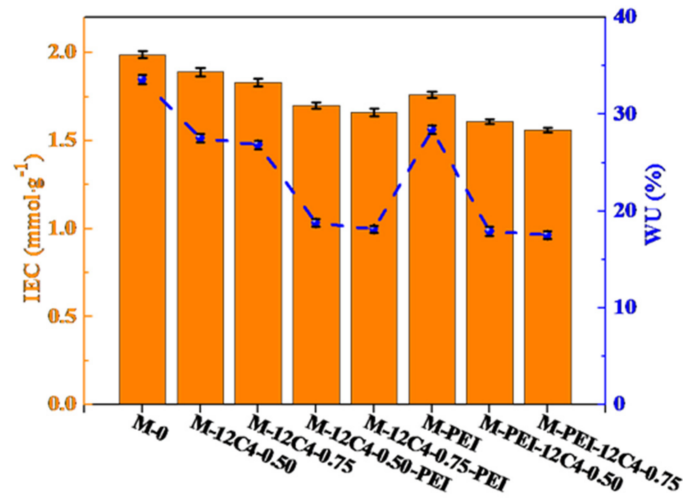


**Figure 5.** IECs and WUs for the pristine (M-0) and modified membranes (M-PEI, M-12C4-x, M-12C4-x-PEI, M-PEI-12C4-x, x = 0.50 and 0.75).
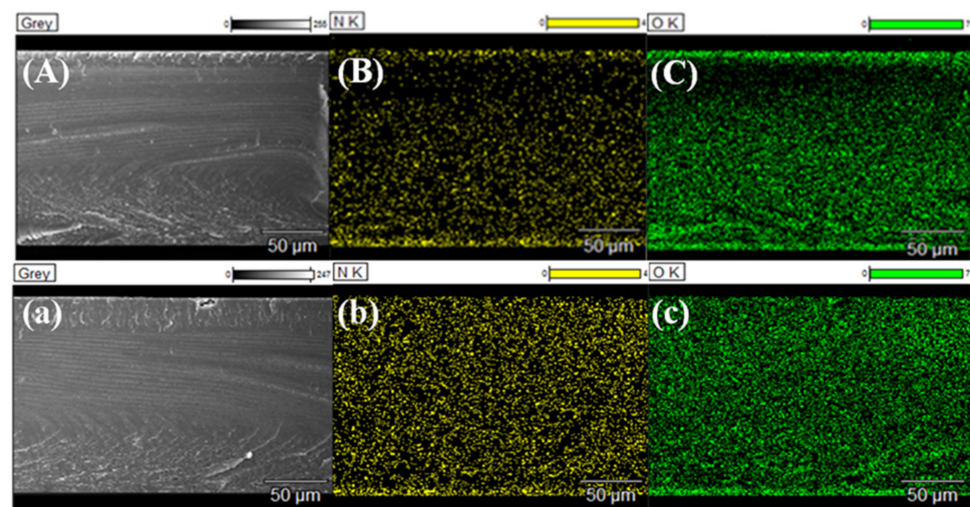


**Figure 6.** EDX elemental maps in the whole cross-section of modified membranes (**A**) M-PEI-12C4-0.75 and (**a**) M-12C4-0.75-PEI (the bottom end of the section is the modified layer), (**B**,**b**) are the N element mapping and (**C**,**c**) are the O element mapping.

*3.3. Electrochemical Properties*

Surface area resistances (R) of the pristine and modified membranes in LiCl and MgCl$_2$ solution were respectively investigated, and the results are presented in Figure 7. It is evident that R values of the modified membranes for one-time deposition (M-PEI, M-12C4-0.50 and M-12C4-0.75) are enhanced relative to M-0 for a given electrolyte solution. Moreover, the R values of two-time coating membranes (M-12C4-x-PEI, M-PEI-12C4-x, x = 0.50 and 0.75) increase remarkably, resulting from the thickened modified layers on the membrane surface and increased modified medium in the membrane matrix. This is in line with the lower IECs and decreased WUs (less free volume), as shown in Figure 5. Furthermore, a great difference of R value occurs in LiCl and MgCl$_2$ solution for a specified membrane. In particular, the resistance difference to MgCl$_2$ and LiCl is significantly obvious for M-12C4-x-PEI (x = 0.50 and 0.75). The hydrated ion radii of Li$^+$ and Mg$^{2+}$ ions are 3.82 and 4.28 Å [44], respectively. In addition, Mg$^{2+}$ shows a lower migration rate and

self-diffusion coefficient in aqueous solution [2]. A PEI/DA coating onto the outermost of membrane is more beneficial to Li$^+$ transfer than Mg$^{2+}$ than a 12C4/DA coating. As a result, it can reflect the selective transport of Li$^+$ vs. Mg$^{2+}$ in a different membrane matrix.
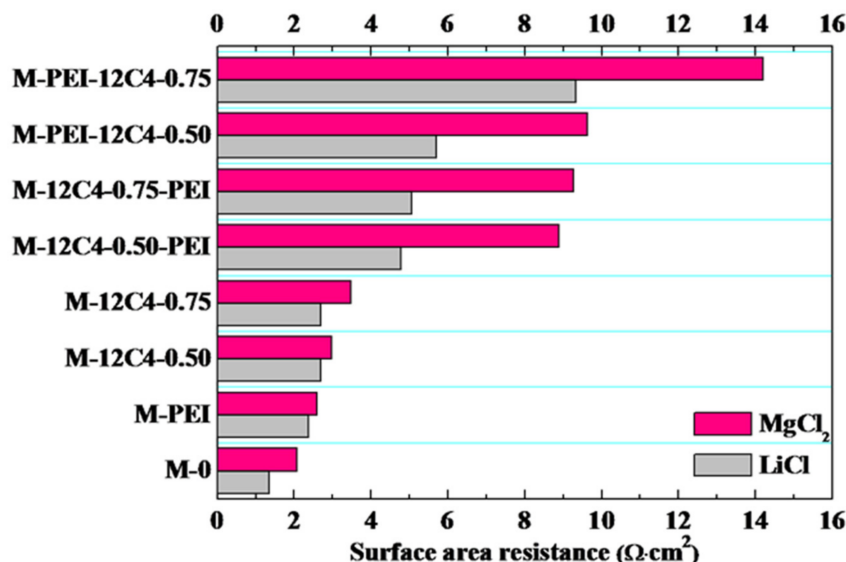


**Figure 7.** Surface area resistances for the pristine (M-0) and modified membranes (M-PEI, M-12C4-x, M-12C4-x-PEI, M-PEI-12C4-x, x = 0.50 and 0.75).

Polarization current–voltage (C–V) curves can provide insight into the ion transport behavior of ion exchange membranes over a range of currents [34]. Figure 8a shows the C–V curves of the pristine and several modified membranes measured in the mixture of 0.05 M LiCl and 0.05 M MgCl$_2$. All the curves exhibit three typical characteristic regions: ohmic region, plateau region, and over-limiting region [34,45,46]. In the ohmic region, it presents a linear dependence between membrane voltage and current density. Moreover, the ohmic resistance (R$_{ohm}$, $\Omega \cdot cm^2$) of the membrane system can be served through the inverse of the slope of the ohmic region. Furthermore, a small current increase leads to large improvement of voltage owing to continuous ion depletion in the diffusion boundary layer, which is followed by a plateau occurrence. The limiting current density ($I_m$, mA·cm$^{-2}$) is determined by the intersection of the ohmic and plateau regions, as the maximum current applied in the membrane system. The membrane voltage further increases linearly with the current density, resulting in an over-limiting region, where water splitting and electroconvection probably appear.
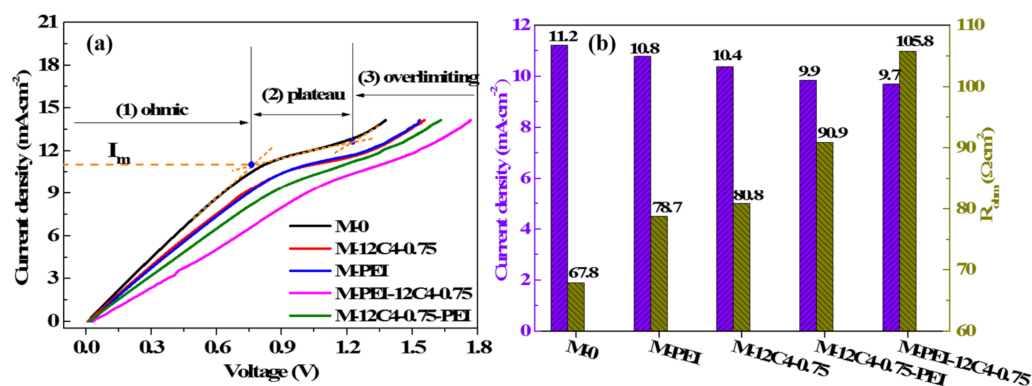


**Figure 8.** Current density–voltage curves (**a**) and systematic ohmic resistances (**b**) for the pristine (M-0) and modified membranes (M-12C4-0.75, M-PEI, M-PEI-12C4-0.75 and M-12C4-0.75-PEI) in 0.05 M binary mixture of LiCl and MgCl$_2$.

We can see in Figure 8b that systematic ohmic resistances for all the modified membranes are higher than that of M-0 (67.8 $\Omega \cdot cm^2$), even reaching the highest value (105.8 $\Omega \cdot cm^2$) for M-PEI-12C4-0.75. It is in accordance with the results of surface area resistance in Figure 7. On the contrary, $I_m$ of the modified membranes varies from 11.2 to 9.7 $mA \cdot cm^{-2}$, relative to M-0 (see from Figure 8b). These phenomena are consistent with some previous reports [20,28,46,47]. It is primarily attributable that the codeposition products on the membrane surface and permeating into the inner part of membrane matrix suppress cation migration to a certain extent [47]. The heterogeneous membrane surface after coating forms part of non-conductive regions, leading to an earlier and faster salt ion depletion in the conductive regions. Hence, a decreased current density is observable [20].

### 3.4. Evaluation of Monovalent Cation Selectivity

To evaluate the selective separation performance of the modified membranes, ED experiments were measured in 0.05 M binary mixture of LiCl and $MgCl_2$. According to the investigation of current–voltage curves, the current density is constant at 5.0 $mA \cdot cm^{-2}$ throughout the tests. Figure 9 shows the permselectivity between $Li^+$ and $Mg^{2+}$ of the pristine and modified membranes. M-0 presents a poor permselectivity to $Li^+$ ions ($P_{Mg^{2+}}^{Li^+} = 0.46$), which is due to the usually larger attraction of the fixed ion exchange sites toward multivalent cations [48]. With the introduction of a codeposition coating of 12C4/DA, the permselectivity of M-12C4-0.75 to $Li^+$ ions is improved up to 1.02. In addition, the modified membrane M-PEI exhibits a higher permselectivity value ($P_{Mg^{2+}}^{Li^+} = 1.74$). Based on these one-time codeposition modified membranes, it is concluded that benzo-12-crown-4 derivatives and PEI respectively introduced on the membrane surface have a remarkably conducive effect on the enhancement of $Li^+$ selectivity in the mixture of $Li^+$ and $Mg^{2+}$ ions. Furthermore, combining the characteristics of benzo-12-crown-4 and PEI, we have further investigated the selective separation performance to $Li^+$ ions of the two-time codeposited membranes. A steep increase in $P_{Mg^{2+}}^{Li^+}$ can be apparently observed in comparison to the one-time codeposited membranes, which confirms the positive effects of two-time modification. Moreover, $P_{Mg^{2+}}^{Li^+}$ values of M-12C4-0.50-PEI (5.23) and M-12C4-0.75-PEI (4.72) are far higher than those of M-PEI-12C4-0.50 (2.46) and M-PEI-12C4-0.75 (2.12). Obviously, the decoration sequence of benzo-12-crown-4 derivative and PEI has a significant influence on $Li^+$ ions separation (the detailed discussion is in Section 3.5).
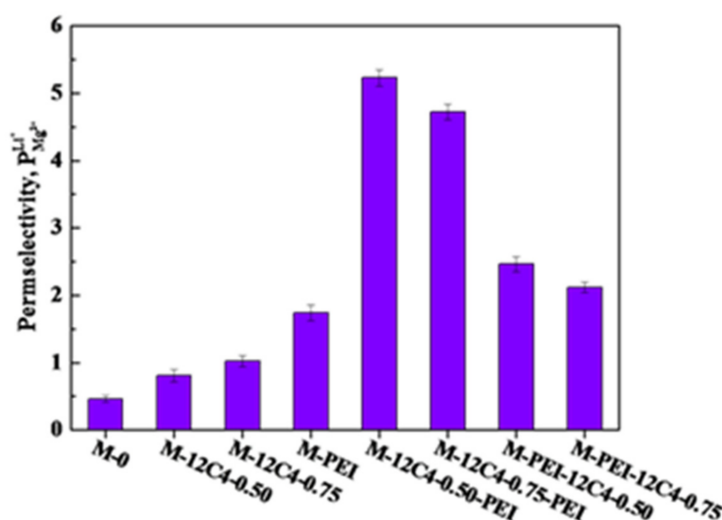


**Figure 9.** Permselectivity for the pristine (M-0) and modified (M-PEI, M-12C4-x, M-12C4-x-PEI, M-PEI-12C4-x, x = 0.50 and 0.75) membranes in 0.05 M binary mixture of LiCl and $MgCl_2$ at current density of 5.0 $mA \cdot cm^{-2}$.

To further investigate the separation performance of modified membranes on other cations, M-12C4-0.50-PEI was chosen to be performed by ED in the mixture of $K^+/Mg^{2+}$ and $K^+/Li^+$. As shown in Figure 10, in $K^+/Mg^{2+}$ system, M-12C4-0.50-PEI presents remarkable permselectivity to $K^+$ ions ($P_{Mg^{2+}}^{K^+} = 13.56$) compared with M-0 ($P_{Mg^{2+}}^{K^+} = 1.23$), which is far higher than those of M-co-0.50 ($P_{Mg^{2+}}^{K^+} = 5.99$) and commercial CIMS ($P_{Mg^{2+}}^{K^+} = 5.36$) reported in our previous work in the same test condition [28]. It can be mainly due to the strong electrostatic repulsion effect of PEI coated on the outermost of the membrane. Whereas, for the separation of $K^+/Li^+$, $P_{K^+}^{Li^+}$ reaches 2.69 for M-12C4-0.50-PEI, which is much higher than those of M-0 (1.18), M-co-0.50 (2.05) and CIMS (1.16). It can be speculated that the dense modified membrane structure restrains the transportation of cations with larger hydrated radii through a pore-size sieving effect.
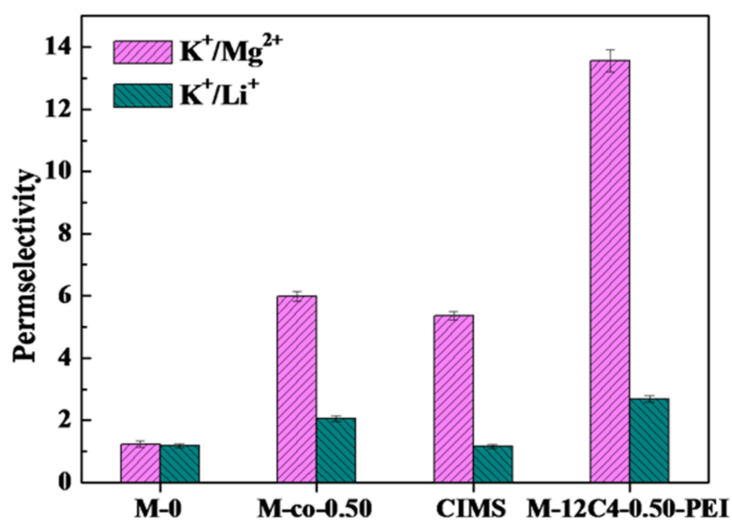


**Figure 10.** Permselectivity for membranes M-0, M-12C4-0.50-PEI, M-co-0.50 and CIMS in 0.05 M binary mixture of $KCl/MgCl_2$ and $KCl/LiCl$ at current density of 5.0 mA·cm$^{-2}$.

*3.5. Analysis of the Effects of Modification Sequence on Cation Permselectivity*

From the investigation of cation permselectivity for the CEMs stated above, we can see the two-time codeposition modified membranes M-12C4-0.50-PEI and M-12C4-0.75-PEI achieve distinct selective separation between binary mixture cations. It is plausibly attributed to three synergistic effects: electrostatic repulsion, ion–dipole interaction between $Li^+$ ions and benzo-12-crown-4 derivatives, as well as pore-size sieving effect. As is expected, the introduction of benzo-12-crown-4 is to provide facile ion channels for $Li^+$ ions, while the presence of positively charged PEI is to inhibit $Mg^{2+}$ ions migration through the membrane via strong electrostatic repulsion toward multivalent cations.

From the results of $Li^+/Mg^{2+}$ separation for one-time codeposited membranes (see Figure 9), it is concluded that the electrostatic repulsion of the PEI coating is more effective than the ion–dipole interaction of 12C4 decorating. Similarly, for the two-time codeposited membranes, PEI coated on the outermost layer plays a dominant role to achieve out-performing permselectivity to $Li^+$ ions; $P_{Mg^{2+}}^{Li^+}$ values are respectively 2.46 and 5.23 for M-PEI-12C4-0.50 and M-12C4-0.50-PEI. Figure 11 presents the different processes of cation selective permeation ($Li^+$ and $Mg^{2+}$) through modified layers of membranes M-12C4-0.50-PEI and M-PEI-12C4-0.50. Cations in the bulk of the dilute side migrate directionally to the interface of modified CEM under the electric field force. For M-12C4-0.50-PEI (see Figure 11a), abundant positively charged amine groups of PEI on the secondary modified layer (PEI/DA) show stronger electrostatic repulsion toward major $Mg^{2+}$ ions relative to $Li^+$ ions. When the remaining cations migrate into the first modified layer (12C4/DA), part of $Li^+$ ions are first dehydrated and then complexed with ether ring of 12C4. The

complexing formations of 12C4 ~Li$^+$ present positive, and they can further suppress the transportation of partial Mg$^{2+}$ ions through electrostatic repulsion. Under the driving of galvanostatic electric field, Li$^+$ ions in complexed form can gradually pass through the membrane [49]. The last but not the least, as stated above, modified medium occupies abundant free space of the membrane matrix, which results in lower WUs (see Figure 5), higher R$_{ohm}$ (see Figure 7), and denser structures. This pore-size sieving effect is conducive to the passing of cations with smaller hydrated radii. However, among the cations on the membrane surface for M-PEI-12C4-0.50, dehydrated Li$^+$ ions are prone to interact with 12C4 on the outer modified layer (12C4/DA), which would slow down the motion of Li$^+$ ions; meanwhile, the migration of Mg$^{2+}$ ions is also partially affected by the positive complexing. Moreover, in addition to reacting with DA on the first modified layer (PEI/DA), the remaining amine groups of PEI are inclined to react with DA from the secondary deposition solution (12C4/DA). It can be speculated that the free positively charged PEI shows relatively weak electrostatic repulsion toward cations. Combined with the electrodialytic performance of one-time modified membranes (M-PEI and M-12C4-0.50), it is not difficult to conclude the prominent electrodialytic permselectivity to Li$^+$ ions in the Li$^+$/Mg$^{2+}$ system for M-12C4-0.50-PEI.
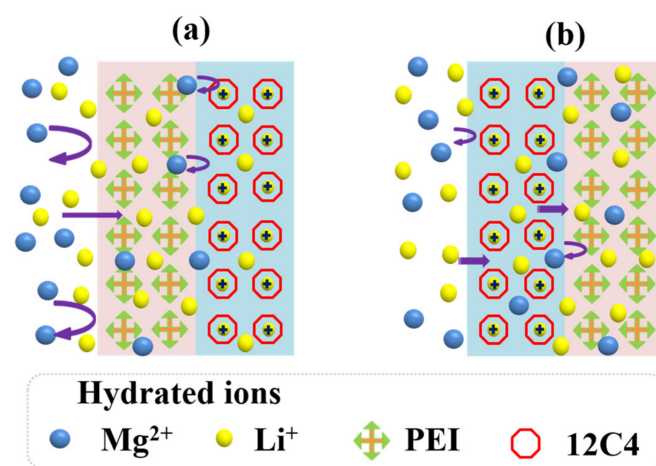


**Figure 11.** Analysis for the selective permeation of cations (Li$^+$ and Mg$^{2+}$) through modified layers of membranes (**a**) M-12C4-0.50-PEI and (**b**) M-PEI-12C4-0.50.

In addition, energy consumption (E) and current efficiency (η) are significant parameters to evaluate the performance of membranes. As shown in Figure 12, M-PEI-12C4-0.50 displays increased E$_{SEC}$ and decreased η values in comparison with M-12C4-0.50-PEI, which is attributed to the reduction in membrane conductivity (lower IECs and WUs shown in Figure 5). A thin rigid coating on membrane surface affects the microstructure of membrane; thus, partial ionic transport is retarded [25,50]. R$_{LiCl}$ and R$_{MgCl2}$ of M-PEI-12C4-0.50 are respectively higher than those of M-12C4-0.50-PEI (see in Figure 7), respectively, which manifests that a more compact membrane structure for M-PEI-12C4-0.50 suppresses the migration of Li$^+$ and Mg$^{2+}$ ions.

Furthermore, due to the smaller hydrated radii of K$^+$ ions compared with Li$^+$ ions, for the separation of K$^+$/Mg$^{2+}$, the synergistic effects of electrostatic repulsion and pore-size sieving effect are more prominent for M-12C4-0.50-PEI.
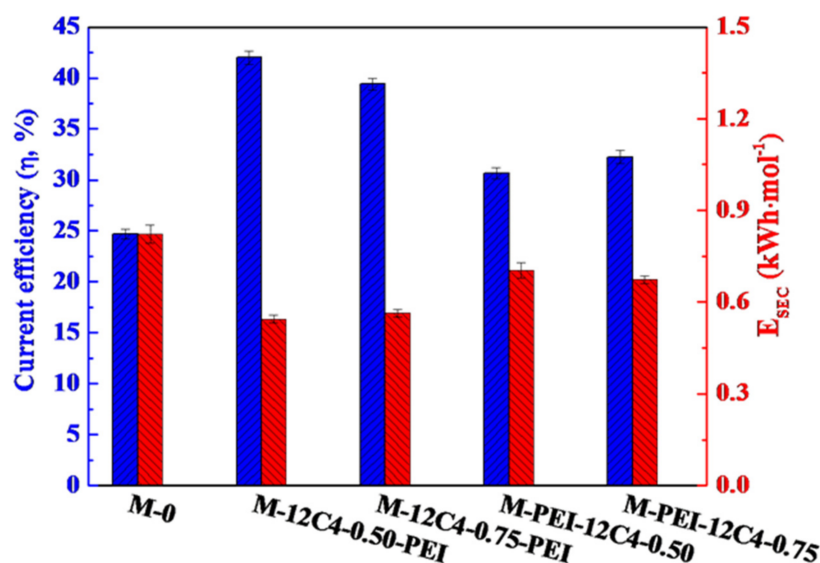
**Figure 12.** Current efficiency ($\eta$) and energy consumption ($E_{SEC}$) of the pristine (M-0) and modified (M-12C4-x-PEI, M-PEI-12C4-x, x = 0.50 and 0.75) membranes in 0.05 M binary mixture of LiCl and MgCl$_2$ at a current density of 5.0 mA·cm$^{-2}$.

## 4. Conclusions

A series of novel monovalent cation perm-selective membranes have been fabricated based on sulfonated polysulfone (SPSF) membrane. By changing the codeposition sequence of PEI/DA and 12C4/DA on the membrane surface, significant differences present in the physicochemical and electrochemical properties as well as the electrodialytic performance of the modified membranes. M-12C4-0.50-PEI exhibited significantly prominent perms-electivity to Li$^+$ ions in the Li$^+$/Mg$^{2+}$ system, which possibly arises from the synergistic effects of electrostatic repulsion (positively charged PEI), pore-size sieving (distribution of modified ingredients) and specific interaction effect (12C4 ~Li$^+$). A higher permselectivity to K$^+$ ions of M-12C4-0.50-PEI is mainly attributable to the strong electrostatic repulsion and pore-size sieving effect, in comparison with M–0. This work can provide a potential approach in separation of specific cations.

**Author Contributions:** Conceptualization, S.Y. (Shanshan Yang) and C.G.; formal analysis, S.Y. (Shanshan Yang); J.S., and C.G.; methodology, S.Y. (Shanshan Yang); writing—original draft, S.Y. (Shanshan Yang); writing—review and editing, S.Y. (Shanshan Yang), S.Y. (Shuaijun Yu), L.Y., Y.L., J.L., J.S., and C.G.; investigation, S.Y. (Shanshan Yang), S.Y. (Shuaijun Yu), and L.Y., Funding acquisition, J.L., J.S., and C.G.; All authors have read and agreed to the published version of the manuscript.

**Institutional Review Board Statement:** Not applicable.

**Informed Consent Statement:** Not applicable.

**Data Availability Statement:** Not applicable.

**Conflicts of Interest:** The authors declare no conflict of interest.

## References

1. Nagarale, R.; Gohil, G.; Shahi, V. Recent developments on ion-exchange membranes and electro-membrane processes. *Adv. Colloid Interface Sci.* **2006**, *119*, 97–130. [PubMed]
2. Luo, T.; Abdu, S.; Wessling, M. Selectivity of ion exchange membranes: A review. *J. Membr. Sci.* **2018**, *555*, 429–454. [CrossRef]
3. Zhou, J.; Jiao, Z.; Zhu, Q.; Li, Y.; Ge, L.; Wu, L.; Yang, Z.; Xu, T. Biselective microporous Tröger's base membrane for effective ion separation. *J. Membr. Sci.* **2021**, *627*, 119246. [CrossRef]
4. White, N.; Misovich, M.; Alemayehu, E.; Yaroshchuk, A.; Bruening, M.L. Highly selective separations of multivalent and monovalent cations in electrodialysis through Nafion membranes coated with polyelectrolyte multilayers. *Polymer* **2016**, *103*, 478–485. [CrossRef]
5. Sata, T.; Sata, T.; Yang, W. Studies on cation-exchange membranes having permselectivity between cations in electrodialysis. *J. Membr. Sci.* **2002**, *206*, 31–60. [CrossRef]
6. Sun, Y.; Wang, Q.; Wang, Y.; Yun, R.; Xiang, X. Recent advances in magnesium/lithium separation and lithium extraction technologies from salt lake brine. *Sep. Purif. Technol.* **2021**, *256*, 117807.
7. Vaselbehagh, M.; Karkhanechi, H.; Takagi, R.; Matsuyama, H. Surface modification of an anion exchange membrane to improve the selectivity for monovalent anions in electrodialysis—Experimental verification of theoretical predictions. *J. Membr. Sci.* **2015**, *490*, 301–310. [CrossRef]
8. Zheng, Z.; Xiao, P.; Ruan, H.; Liao, J.; Gao, C.; Van der Bruggen, B.; Shen, J. Mussel-inspired surface functionalization of AEM for simultaneously improved monovalent anion selectivity and antibacterial property. *Membranes* **2019**, *9*, 36. [CrossRef]
9. Wang, W.; Liu, R.; Tan, M.; Sun, H.; Niu, Q.J.; Xu, T.; Nikonenko, V.; Zhang, Y. Evaluation of the ideal selectivity and the performance of selectrodialysis by using TFC ion exchange membranes. *J. Membr. Sci.* **2019**, *582*, 236–245. [CrossRef]
10. Sata, T. Modification of properties of ion-exchange membranes. IV. Change of transport properties of cation-exchange membranes by various polyelectrolytes. *J. Polym. Sci. Polym. Chem. Ed.* **1978**, *16*, 1063–1080. [CrossRef]
11. Sata, T.; Tanimoto, M.; Kawamura, K.; Matsusaki, K. Transport properties of cation exchange membranes in the presence of ether compounds in electrodialysis. *J. Colloid Interface Sci.* **1999**, *219*, 310–319. [CrossRef] [PubMed]
12. He, G.; Li, Z.; Zhao, J.; Wang, S.; Wu, H.; Guiver, M.D.; Jiang, Z. Nanostructured ion-exchange membranes for fuel cells: Recent advances and perspectives. *Adv. Mater.* **2015**, *27*, 5280–5295. [CrossRef]
13. Irfan, M.; Xu, T.; Ge, L.; Wang, Y.; Xu, T. Zwitterion structure membrane provides high monovalent/divalent cation electrodialysis selectivity: Investigating the effect of functional groups and operating parameters. *J. Membr. Sci.* **2019**, *588*, 117211. [CrossRef]
14. Liao, J.; Yu, X.; Chen, Q.; Gao, X.; Ruan, H.; Shen, J.; Gao, C. Monovalent anion selective anion-exchange membranes with imidazolium salt-terminated side-chains: Investigating the effect of hydrophobic alkyl spacer length. *J. Membr. Sci.* **2020**, *599*, 117818. [CrossRef]
15. Partridge, A.; Milestone, C.; Too, C.; Wallace, G. Polypyrrole based cation transport membranes. *J. Membr. Sci.* **1999**, *152*, 61–70. [CrossRef]
16. Gohil, G.S.; Binsu, V.V.; Shahi, V.K. Preparation and characterization of mono-valent ion selective polypyrrole composite ion-exchange membranes. *J. Membr. Sci.* **2006**, *280*, 210–218. [CrossRef]
17. Farrokhzad, H.; Darvishmanesh, S.; Genduso, G.; Van Gerven, T.; Van der Bruggen, B. Development of bivalent cation selective ion exchange membranes by varying molecular weight of polyaniline. *Electrochim. Acta* **2015**, *158*, 64–72. [CrossRef]
18. Falina, I.; Loza, N.; Loza, S.; Titskaya, E.; Romanyuk, N. Permselectivity of Cation Exchange Membranes Modified by Polyaniline. *Membranes* **2021**, *11*, 227. [CrossRef] [PubMed]
19. Amara, M.; Kerdjoudj, H. Modification of cation-exchange membrane properties by electro-adsorption of polyethyleneimine. *Desalination* **2003**, *155*, 79–87. [CrossRef]
20. Wang, M.; Liu, X.; Jia, Y.; Wang, X. The improvement of comprehensive transport properties to heterogeneous cation exchange membrane by the covalent immobilization of polyethyleneimine. *Sep. Purif. Technol.* **2015**, *140*, 69–76. [CrossRef]
21. Li, J.; Zhou, M.; Lin, J.; Ye, W.; Xu, Y.; Shen, J.; Gao, C.; Bruggen, B. Mono-valent cation selective membranes for electrodialysis by introducing polyquaternium-7 in a commercial cation exchange membrane. *J. Membr. Sci.* **2015**, *486*, 89–96. [CrossRef]
22. Hu, Y.; Wang, M.; Wang, D.; Gao, X.; Gao, C. Feasibility study on surface modification of cation exchange membranes by quaternized chitosan for improving its selectivity. *J. Membr. Sci.* **2008**, *319*, 5–9. [CrossRef]
23. Wang, M.; Jia, Y.; Yao, T.; Wang, K. The endowment of monovalent selectivity to cation exchange membrane by photo-induced covalent immobilization and self-crosslinking of chitosan. *J. Membr. Sci.* **2013**, *442*, 39–47. [CrossRef]
24. Li, J.; Yuan, S.; Wang, J.; Zhu, J.; Shen, J.; Bruggen, B. Mussel-inspired modification of ion exchange membrane for monovalent separation. *J. Membr. Sci.* **2018**, *553*, 139–150. [CrossRef]
25. Thakur, A.K.; Manohar, M.; Shahi, V.K. Controlled metal loading on poly(2-acrylamido-2-methyl-propane-sulfonic acid) membranes by an ion-exchange process to improve electrodialytic separation performance for mono-/bi-valent ions. *J. Mater. Chem. A* **2015**, *3*, 18279–18288. [CrossRef]
26. Greben, V.; Rodzik, I. Difference in transfer of magnesium and sodium ions through electrodialytic membranes modified with chitosan. *Russ. J. Appl. Chem.* **2008**, *81*, 412–414. [CrossRef]
27. Pang, X.; Tao, Y.; Xu, Y.; Pan, J.; Shen, J.; Gao, C. Enhanced monovalent selectivity of cation exchange membranes via adjustable charge density on functional layers. *J. Membr. Sci.* **2020**, *595*, 117544. [CrossRef]

28. Yang, S.; Liu, Y.; Liao, J.; Liu, H.; Jiang, Y.; Van der Bruggen, B.; Shen, J.; Gao, C. Codeposition modification of cation exchange membranes with dopamine and crown ether to achieve high K+ electrodialysis selectivity. *ACS Appl. Mater. Interfaces* **2019**, *11*, 17730–17741. [CrossRef] [PubMed]

29. Sata, T.; Kawamura, K.; Higa, M.; Matsusaki, K. Electrodialytic transport properties of cation exchange membranes. *J. Membr. Sci.* **2001**, *183*, 201–212. [CrossRef]

30. Xu, P.; Hong, J.; Qian, X.; Xu, Z.; Xia, H.; Tao, X.; Xu, Z.; Ni, Q. Materials for lithium recovery from salt lake brine. *J. Mater. Sci.* **2020**, *56*, 16–63.

31. Tripathi, G.; Ramanathan, G. Crystallographic studies on complexes of potassium iodide and copper perchlorate with N, N′-dicyclohexylurea tethered to a benzo-12-crown-4. *J. Mol. Struct.* **2018**, *1156*, 273–279. [CrossRef]

32. Steed, J. First- and second-sphere coordination chemistry of alkali metal crown ether complexes. *Coord. Chem. Res.* **2001**, *215*, 171–221. [CrossRef]

33. Ali, M.; Ahmed, I.; Ramirez, P.; Nasir, S.; Mafe, S.; Niemeyer, C.M.; Ensinger, W. Lithium ion recognition with nanofluidic diodes through host–guest complexation in confined geometries. *Anal. Chem.* **2018**, *90*, 6820–6826. [CrossRef]

34. Abdu, S.; Martí-Calatayud, M.; Wong, J.; García-Gabaldón, M.; Wessling, M. Layer-by-layer modification of cation exchange membranes controls ion selectivity and water splitting. *ACS Appl. Mater. Interfaces* **2014**, *6*, 1843–1854. [CrossRef]

35. Lee, H.; Dellatore, S.M.; Miller, W.M.; Messersmith, P.B. Mussel-Inspired Surface Chemistry for Multifunctional Coatings. *Science* **2007**, *318*, 426–430. [CrossRef] [PubMed]

36. Cuartero, M.; Crespo, G.A.; Bakker, E. Ionophore-Based Voltammetric Ion Activity Sensing with Thin Layer Membranes. *Anal. Chem.* **2016**, *88*, 1654–1660. [CrossRef] [PubMed]

37. Chen, Q.; Ji, Z.; Liu, J.; Zhao, Y.; Wang, S.; Yuan, J. Development of recovering lithium from brines by selective-electrodialysis: Effect of coexisting cations on the migration of lithium. *J. Membr. Sci.* **2018**, *548*, 408–420. [CrossRef]

38. Devrim, Y.; Erkan, S.; Baç, N.; Eroğlu, I. Preparation and characterization of sulfonated polysulfone/titanium dioxide composite membranes for proton exchange membrane fuel cells. *Int. J. Hydrogen Energy* **2009**, *34*, 3467–3475. [CrossRef]

39. Lv, Y.; Yang, H.; Liang, H.; Wan, L.; Xu, Z. Nanofiltration membranes via co-deposition of polydopamine/polyethylenimine followed by cross-linking. *J. Membr. Sci.* **2015**, *476*, 50–58. [CrossRef]

40. Zhang, R.; Su, Y.; Zhao, X.; Li, Y.; Zhao, J.; Jiang, Z. A novel positively charged composite nanofiltration membrane prepared by bio-inspired adhesion of polydopamine and surface grafting of poly(ethylene imine). *J. Membr. Sci.* **2014**, *470*, 9–17. [CrossRef]

41. Kasprzak, A.; Poptawska, M.; Bystrzejewski, M.; Labedz, O.; Grudzinski, I. Conjugation of polyethylenimine and its derivatives to carbon-encapsulated iron nanoparticles. *RSC Adv.* **2015**, *5*, 85556–85567. [CrossRef]

42. Zhang, H.; Li, X.; Zhao, C.; Fu, T.; Shi, Y.; Na, H. Composite membranes based on highly sulfonated PEEK and PBI: Morphology characteristics and performance. *J. Membr. Sci.* **2008**, *308*, 66–74. [CrossRef]

43. Luo, H.; Agata, W.; Geise, G. Connecting the ion separation factor to the sorption and diffusion selectivity of ion exchange membranes. *Ind. Eng. Chem. Res.* **2020**, *59*, 14189–14206. [CrossRef]

44. Nightingale, E. Phenomenological theory of ion solvation. Effective radii of hydrated ions. *J. Chem. Phys.* **1959**, *63*, 1381–1387. [CrossRef]

45. White, N.; Misovich, M.; Yaroshchuk, A.; Bruening, M.L. Coating of Nafion Membranes with Polyelectrolyte Multilayers to Achieve High Monovalent/Divalent Cation Electrodialysis Selectivities. *ACS Appl. Mater. Interfaces* **2015**, *7*, 6620–6628. [CrossRef]

46. Chamoulaud, G.; Bélanger, D. Modification of ion-exchange membrane used for separation of protons and metallic cations and characterization of the membrane by current–voltage curves. *J. Colloid Interface Sci.* **2005**, *281*, 179–187. [CrossRef] [PubMed]

47. Yao, T.; Wang, M.; Jia, Y.; Zhou, P. A modified coating method for preparing a mono-valent perm-selective cation exchange membrane: I. The evolution of membrane property corresponding to different preparing stages. *Desalin. Water Treat.* **2013**, *51*, 2740–2748. [CrossRef]

48. Chapotot, A.; Pourcelly, G.; Gavach, C. Transport competition between monovalent and divalent cations through cation-exchange membranes. Exchange isotherms and kinetic concepts. *J. Membr. Sci.* **1994**, *96*, 167–181. [CrossRef]

49. Chaudhury, S.; Bhattacharyya, A.; Goswami, A. Electrodriven Ion Transport through Crown Ether–Nafion Composite Membrane: Enhanced Selectivity of Cs+ over Na+ by Ion Gating at the Surface. *Ind. Eng. Chem. Res.* **2014**, *53*, 8804–8809. [CrossRef]

50. Luo, T.; Roghmans, F.; Wessling, M. Ion mobility and partition determine the counter-ion selectivity of ion exchange membranes. *J. Membr. Sci.* **2020**, *597*. [CrossRef]